frontiers | Frontiers in Physics

BRIEF RESEARCH REPORT
published: 25 April 2022
doi: 10.3389/fphy.2022.841413

Impact of Fabrication Processes of Small-Molecule-Doped Polymer Thin-Films on Room-Temperature Phosphorescence

*Heidi Thomas[1], Katherina Haase[2], Tim Achenbach[1], Toni Bärschneider[1], Anton Kirch[1], Felix Talnack[2], Stefan C. B. Mannsfeld[2] and Sebastian Reineke[1]**

[1]*Dresden Integrated Center for Applied Physics and Photonic Materials (IAPP), Technische Universität Dresden, Dresden, Germany,* [2]*Center for Advancing Electronics Dresden (cfaed) and Faculty of Electrical and Computer Engineering, Technische Universität Dresden, Dresden, Germany*

The development of organic materials displaying room-temperature phosphorescence is a research field that has attracted more and more attention in the last years. Most studies focus on designing or optimizing emitter molecules to increase the phosphorescent performance in host:emitter systems. Rarely, the overall thin-film preparation routines are compared with respect to their triplet-state luminescence yield. Herein, different film preparation techniques are investigated using the very same emitter molecule. A variation of host polymer, post-annealing temperature, and fabrication procedure is evaluated with respect to the obtained phosphorescent lifetime, photoluminescent quantum yield, and phosphorescence-to-luminescence ratio. This study elaborates the importance of different film preparation techniques and gathers a concise set of data which is helpful to anyone optimizing the phosphorescence of a particular system.

Keywords: room-temperature phosphorescence, host-guest system, wet thin-film processing, persistent phosphorescence, UV excitation, persistent luminescence, organic emitter, triplet state

OPEN ACCESS

Edited by:
Rene A. Nome,
State University of Campinas, Brazil

Reviewed by:
Zhenghuan Lin,
Fujian Normal University, China
Ahmed Al-Masoodi,
American University of Kurdistan, Iraq

****Correspondence:***
Sebastian Reineke
sebastian.reineke@tu-dresden.de

Specialty section:
This article was submitted to Physical Chemistry and Chemical Physics, a section of the journal Frontiers in Physics

Received: *22 December 2021*
Accepted: *01 April 2022*
Published: *25 April 2022*

Citation:
Thomas H, Haase K, Achenbach T, Bärschneider T, Kirch A, Talnack F, Mannsfeld SCB and Reineke S (2022) Impact of Fabrication Processes of Small-Molecule-Doped Polymer Thin-Films on Room-Temperature Phosphorescence. Front. Phys. 10:841413. doi: 10.3389/fphy.2022.841413

1 INTRODUCTION

Organic room temperature phosphorescence (RTP), an optical phenomenon originating from the radiative transition of molecular excitations from the triplet excited state to the ground state, has attracted a lot of interest among scientists [1–4]. Its use in information and optical storage, bio-imaging, data encryption, as well as organic light-emitting diodes (OLEDs), and displays [5–12] makes this group of materials indispensable nowadays. To achieve efficient organic RTP, both a substantial intersystem crossing (ISC) between the lowest singlet and the triplet state manifold, as well as the effective suppression of the non-radiative relaxations of triplet excitons are essential [13–15].

According to Yan et.al, [3] one of the key parameters to efficient phosphorescence is the phosphorescence lifetime. There are several pathways to increase it. Among those, host-guest doping [16–18], crystal engineering [19, 20], H-aggregation [21–23], metal-organic and supramolecular frameworks [24, 25], self-assembly [26], as well as luminescent polymers [14, 27–29], and carbon dots [30, 31], just to name a few, can be found. However, phosphorescence is not only characterized by the excited triplet state lifetime, but also by its photoluminescence quantum yield (PLQY) and the phosphorescence-to-luminescence (P2L) ratio (defined later in the text).

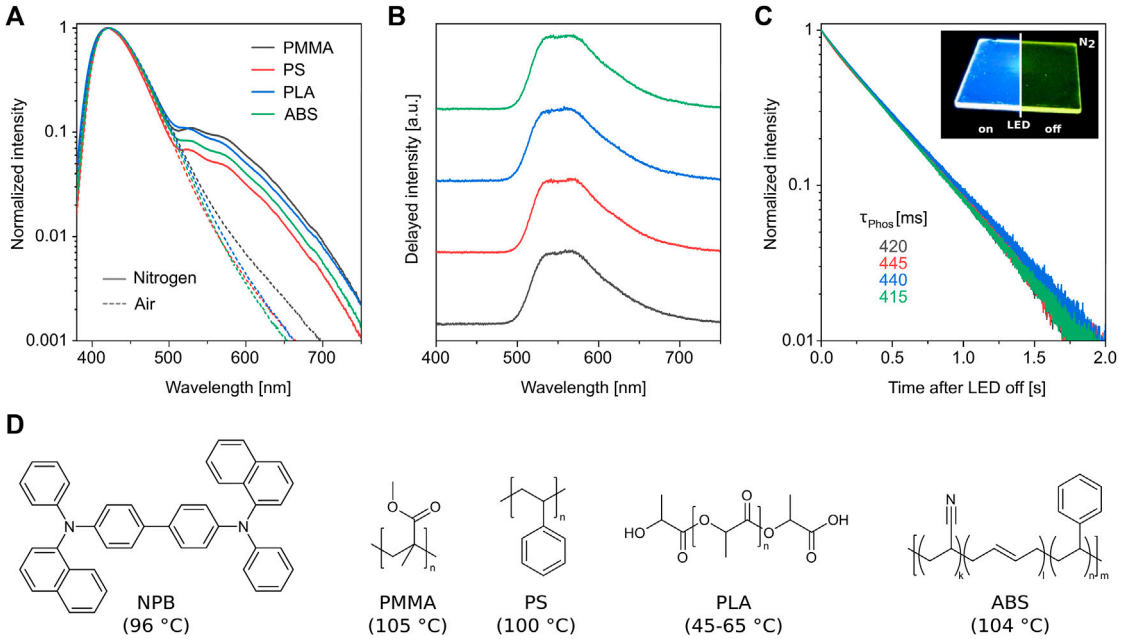

FIGURE 1 | (A) Continuous wave (cw) emission spectra of drop-cast host:NPB films in air (dashed line) and nitrogen atmosphere (solid line). **(B)** Delayed emission spectra showing the respective phosphorescence. **(C)** Phosphorescence decays and lifetimes, inset: PMMA:NPB sample excited with 365 nm showing blue prompt and green delayed emission. **(D)** Molecular structures of NPB and the host polymers used in this work, glass transition temperatures of the polymers given in brackets.

Numerous research groups focused on improving these parameters by employing specially designed emitter molecules like boronic acid esters or carbazoles or rigid polymer matrices such as cyclodextrines [3, 4]. It is, however, equally important to optimize the phosphorescence lifetime, P2L ratio, and PLQY for already existing emitters. This is particularly interesting when different RTP applications may require different processing techniques. It then needs to be elaborated how employing different processing might alter the phosphorescence performance. For fabricating thin films where the emitter is embedded in a polymer matrix, there are a few adjusting screws that can be turned. On the one hand, the nature of the polymer can be important. Polarity, chain length, and side groups can not only promote the interaction of the emitter with the polymer but also rigidify the polymer itself, e.g., by forming intermolecular hydrogen bonds [32, 33] or by a denser packing [1]. This leads to a reduction of the non-radiative decay rate, thus enhancing the phosphorescence lifetime and efficiency. On the other hand, the same effect might probably be achieved by varying the deposition technique since for slower or directed deposition, the packing density can be increased [34]. A similar behavior can be expected by thermal post-treatment of the films [35].

In this report, we study the interplay of the process parameters, host materials, deposition and post-treatment techniques regarding their impact on phosphorescence lifetime, P2L ratio, and PLQY. We utilize a poly (methyl methacrylate) (PMMA):*N,N′*-di (1-naphthyl)-*N,N′*-diphenyl-(1,1′-biphenyl)-4,4′-diamine (NPB) blend as the material system benchmark, as our group has used it extensively throughout the recent years. We developed rewritable photoluminescent tags, PLTs [6], synthesized microparticles [36], and prooved dual-state Förster Resonance Energy Transfer [37] using that system.

2 RESULTS AND DISCUSSION

The thin films studied in this report are comprised of PMMA, polystyrene (PS), polylactic acid (PLA), or acrylonitrile butadiene styrene (ABS) (**Figure 1D**) as host materials and two weight percent (wt%) NPB as guest molecule. The latter is not only a well-known hole transport material in OLED technology [38–40] but also a widely used phosphorescent emitter when embedded into a polymer matrix [37, 41]. We used either spin-coating (sc), drop-casting (dc), or blade-coating (bc) onto quartz substrates under ambient conditions as deposition techniques. The samples were either used as fabricated or were subject to additional post-treatment annealing at 40, 60, 80, 100, or 120°C, respectively, for 24 h in ambient air. These temperatures have been chosen to identify potential changes in the material system exceeding a certain threshold. During this heating step (unheated films were subject to a 24 h waiting time), the films were allowed to reorganize/find their equilibrium over a longer period of time. Except for PLA, the glass transition temperatures (T_G, see **Figure 1D**) are around 100°C. We have chosen the post-annealing temperature range to span from room temperature to slightly above T_G. A further increase in temperature leads to the decomposition of the emitter first, closely followed by the polymer decomposition. PMMA for example starts to

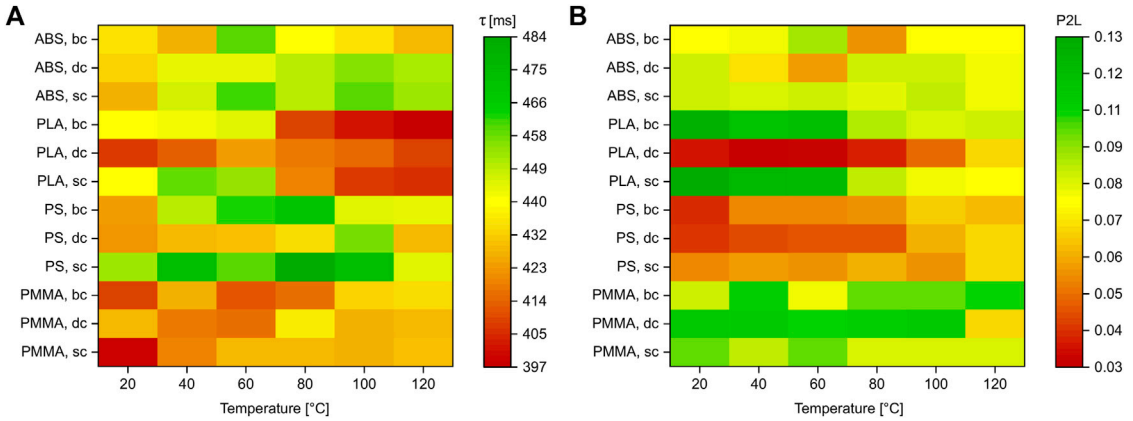

FIGURE 2 | Heat maps of **(A)** phosphorescence lifetime (τ) and **(B)** phosphorescence-to-luminescence ratio (P2L) of spin-coated (sc), drop-cast (dc) as well as blade-coated (bc) polymer:NPB samples for different post annealing temperatures.

decompose already at 180°C. For all 72 samples, the emission spectra in air and nitrogen, as well as the PLQY were measured under 365 nm excitation. The phosphorescence lifetime τ was determined from the transient of the delayed emission (see **Supplementary Tables S1, S2**).

Figure 1 exemplarily shows the spectra of blade-coated samples post-treated at 40°C. In ambient conditions (**Figure 1A**, dashed line), only the blue fluorescence with a peak wavelength of 420 nm is visible, since the phosphorescence is quenched by oxygen [6, 42, 43]. In nitrogen atmosphere (**Figure 1A**, solid line), the green phosphorescence with maximum intensity at 555 nm appears. Taking delayed spectra of the films shows the isolated phosphorescence spectrum (**Figure 1B**). The inset in **Figure 1C** shows a photograph of such a sample during excitation and shortly after the LED is turned off. The lifetimes of the latter are given in **Figure 1C**.

To identify the P2L values, the integral of the emission curves in air (fluorescence, F_{air}) and nitrogen (fluorescence + phosphorescence, $F_{N2} + P = L$) between 380 and 800 nm were determined. With $(L\text{-}F_{air})/L$, the P2L ratio can be calculated. Here, the spectra in nitrogen were recorded at low excitation intensities to prevent nonlinear effects such as singlet-triplet annihilation (STA), triplet-triplet annihilation (TTA) [44], and excited-state saturation. PLQY was measured in an integrating sphere at 340 nm excitation. More details of the procedure are given in the supplementary material. **Figure 2** gives an overview of the measurement results.

2.1 Phosphorescence Lifetime

Figure 2A shows the phosphorescence lifetime (τ) of the samples after the respective temperature treatment (see **Supplementary Table S1**). In a first experiment (**Supplementary Table S2**), we used an equal polymer concentration for all three deposition techniques. Here, the spin-coated samples were about ten times thinner than the one of drop-cast or blade-coated samples [e.g., for PMMA samples: 210 nm (sc), 3,150 nm (dc), and 1,835 nm (bc)]. For that reason, we prepared samples by spin-coating with film thicknesses in the range of 150–5,600 nm and measured the respective phosphorescence lifetime. **Supplementary Figure S2** shows, that there is an increase of the lifetime with increasing film thickness.

We therefore decided to increase the film thickness by a second spin-coating series with higher polymer concentration to match the film thickness values of the other coating techniques. Here, we adjusted the film thickness to be in between the ones obtained by drop-casting and blade-coating. Analyzing this series we found that the lifetimes of the thin spin-coated samples are around 15 ms (PMMA), 140 ms (PS), 80 ms (PLA), and 50 (ABS) ms shorter, in case of unheated substrates, compared to the thicker samples.

It has been shown before that polymer chains align during the drying process following a drop-casting or blade-coating fabrication [45]. This change of the nanostructure might influence the overall luminescence and the phosphorescence in particular by decreasing the non-radiative rates. The slow process usually leads to more ordered and less defective films as compared to spin-coated ones. Also, blade-coating can facilitate molecule alignment through applied directional shear stress and likewise results in less defective films with enhanced structural order [46]. As already mentioned, an increase in stiffness of the polymer and consequent suppression of non-radiative rates is supposed to increase the phosphorescence lifetime. We, therefore, performed GIWAXS measurements of samples with PS in order to observe if the different processing methods change the packing of either the NPB or the PS matrix. A summary of the collected data is shown in **Supplementary Figure S3**. For all PS:NPB films we observe a broad ring located at q ~ 1.38 $Å^{-1}$ that we associate with the polystyrene matrix. The corresponding real space distance is approximately 4.55 Å, which coincides with the PS monomer length and thus the average distance of the phenyl rings in PS. Due to the intense, broad scattering signal of the PS matrix, and the tendency to form amorphous films, no scattering signal of NPB could be observed for the PS:NPB films. However, compared to a plain PS film, slight changes in the PS matrix are seen in the blended films, with

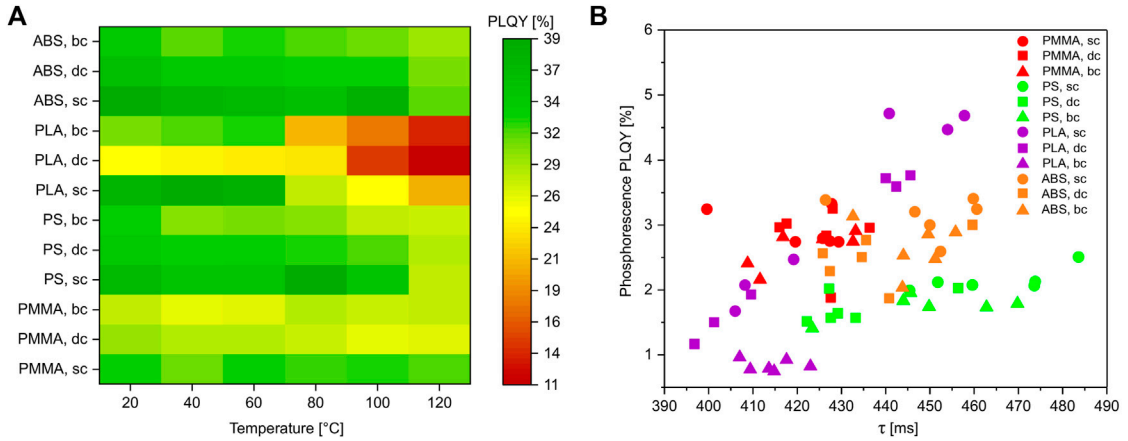

FIGURE 3 | (A) Heat map of PLQY of spin-coated (sc), drop-cast (dc) as well as blade-coated (bc) polymer:NPB samples for different post annealing temperatures. **(B)** Correlation of phosphorescence PLQY and τ for spin-coated (dot), drop-cast (square), and blade-coated (triangle) samples of NPB in PMMA (red), PS (green), PLA (purple), and ABS (orange), respectively.

the PS ring position shifting to smaller q-values. We think that the addition of NPB increases the distance between the phenyl rings, either by a coordination of the NPB molecules at positions in-between the PS phenyl rings or by an increase of the PS chain curvature (**Supplementary Figure S3**). This change of the PS matrix scattering signal also shows that the NPB molecules are well dispersed in the PS matrix and that no phase separation occurs. Furthermore, the position of the ring in the GIWAXS images seems to depend on the processing technique with the most evident change occurring for the drop-cast samples. One may speculate that this trend correlates with the processing and film formation velocity, respectively. Indeed, the deposition time is longest in the case of drop-casting, since the solvent needs several hours to evaporate.

Upon heating of the samples after the deposition, the lifetimes show only an increase of up to 20 ms for drop-cast and blade-coated samples. In addition, there is nearly no change for the thin spin-coated PMMA samples. The glass transition temperatures (T_G) of the used polymers are around 100°C, except for PLA (50–80°C). Up to this temperature, the lifetimes are more or less in the same range. By reaching T_G, they start to decrease which is most prominent for the whole PLA series as well as for thin spin-coated ABS and PS samples. It is remarkable though, that by heating the thick spin-coated samples, the lifetime can be increased by impressive 50 ms (PMMA, 80 and 100°C), 230 ms (PS, 40°C), 250 ms (PLA, 100°C), and 135 ms (ABS, 100°C), compared to the corresponding thin samples. A possible reason could be remaining solvent that was trapped in between the unordered polymer chains and can be released only by heating of the film. It is possible that the order of the chains and the stiffness of the film does not necessarily correlate. In case of spin-coating, the chains are very much unordered but nevertheless the film could be very stiff if the remaining solvent is removed. On the other hand, the ordered chains in drop-cast and blade-coated films might be less stiff due to flexible intermolecular hydrogen bonds.

2.2 Phosphorescence-to-Luminescence Ratio

The phosphorescence-to-luminescence ratio (P2L) indicates the proportion of the phosphorescence in the total emission. This is not only interesting in the case of afterglow applications but also for the visibility of the phosphorescence in continuous wave (cw) photoluminescence in nitrogen atmosphere. If the P2L ratio is over 0.5, the intensity of the phosphorescence is higher than the one of the fluorescence, thus enabling the detection of the phosphorescence signal clearly by eye even under cw illumination [47, 48].

From the data presented in **Figure 2B** we cannot deduce any systematic influence of post-annealing or fabrication technique, but it can be shown, that PS as well as the drop-cast PLA samples show the lowest P2L ratio.

2.3 Photoluminescence Quantum Yield

The PLQY is the ratio of emitted to absorbed photons and is quantified in photoluminescence experiments [49]. **Figure 3A** depicts the PLQY values of the samples and looks very similar to **Figure 2A**. By multiplication of the P2L with the PLQY values, the phosphorescence PLQY ($PLQY_{phos}$) can be obtained. **Figure 3B** shows that $PLQY_{phos}$ correlates with the phosphorescence lifetime. This behavior seems to have different trends for each of the tested polymer hosts. We therefore account it to the suppression of non-radiative triplet decay, which influences both the PLQY and lifetime of the excited state and is mediated by the host polymer.

2.4 Global Phosphorescence Performance

To achieve an overall and easy-to-read figure of merit, we define a parameter called global phosphorescence performance (GPP). Each parameter set (phosphorescence lifetime, P2L ratio, and PLQY) is normalized to [0:1], which gives 1 for the best and 0 for the worst value. For each sample, the values of the three

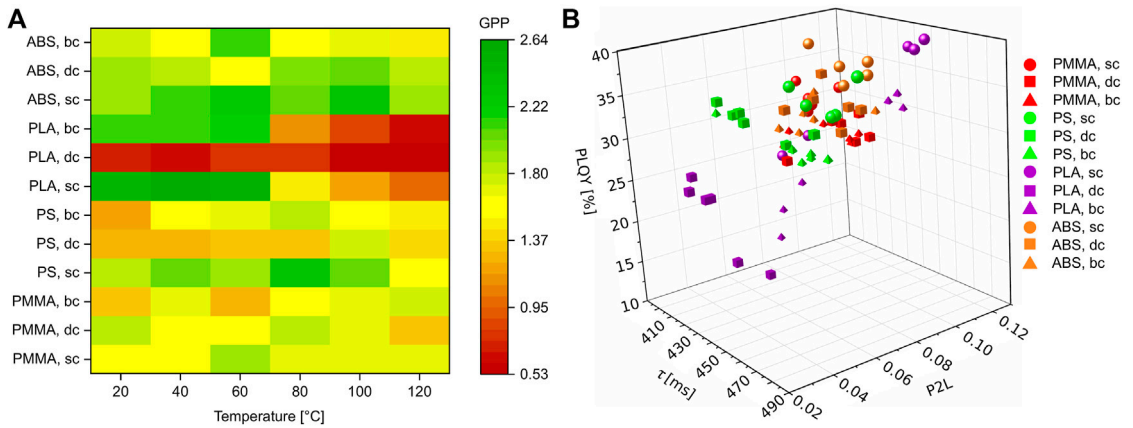

FIGURE 4 | (A) Heat map of the global phosphorescence performance for all 72 samples. **(B)** The same data shown as 3D plot.

parameters were added up, resulting in a score between 0 and 3. The overall GPP for each sample is shown in **Figure 4A** as a heat map and in **Figure 4B** as 3D plot. For the sake of clarity, we decided to not mark each individual point with the respective temperature. The GPP values are provided in **Supplementary Table S1**. As can be seen, there are three PLA samples (purple spheres) in the top-right corner of the plot, indicating the highest GPP. The values correspond to the spin-coated samples post-treated at 40 and 60°C, as well as the untreated one.

Another parameter that might be important is the chain length of the polymeric hosts. Shorter chains might form a denser packing, thus increasing the lifetime by suppressing the non-radiative rates. We have chosen PS with five different chain lengths and four types of PMMA (see **Supplementary Figure S4**). However, there were no dependencies observable. We repeated the same experiment with a different emitter [4,4′-bis(diethylphosphonomethyl)biphenyl (BDPB)] which is known to interact with PMMA by forming intermolecular hydrogen bonds [50], confirming that the lifetime indeed increases with decreasing the PMMA chain length (see **Supplementary Figure S5**). This indicates that NPB does not interact with the polymer matrix in the same way and without measurable changes.

3 MATERIALS AND METHODS

3.1 Chemicals

NPB and PS [MW 280,000 (photophysical measurements) and 35,000 (GIWAXS)] were purchased from Sigma Aldrich, PMMA (MW 550,000) as well as anisole from Alfa Aesar, PLA and ABS from Smart Advanced Systems GmbH.

3.2 Film Fabrication

Both emitter and respective polymer were dissolved in anisole to reach a solution containing 2 wt% NPB and 98 wt% polymer. The polymer concentration was 40 mg/ml (PMMA) and 80 mg/ml (PS, PLA, ABS), respectively. For thick spin-coated samples, concentrations of 120 (PMMA), 250 (PS), 110 (PLA), and 220 mg/ml were used. Cleaned quartz glass substrates of a size of 25 mm by 25 mm were used.

3.2.1 Spin-Coating

A spin coater SCE-150 from Novocontrol Technologies was used. 150 µL of the respective solution was applied to a quartz substrate and spun at 33 rps for 60 s with a ramp of 3 s in case of thin films. The thick films were spun at 20 rps for 180 s.

3.2.2 Drop-Casting

50 µL of the respective solution has been drop-cast onto the quartz substrate and was kept at ambient conditions over night for the solvent to evaporate.

3.2.3 Blade-Coating

Blade coating was carried out with a home-build coating setup consisting of a sample stage that can be heated and a movable blade. The ODTMS-treated [51] blade was kept at a substrate-blade distance of 100 µm with an angle of 8°. All samples were coated with 25 µl at 30 mm/s at normal ambient conditions in air. After coating, they were kept on a hotplate at 40°C for 5 min.

3.2.4 Post-Annealing

To heat the samples to a defined temperature, a hotplate VWR VMS-C7 was used. A 160 × 160 × 10 mm aluminum block with 16 squares (30 × 30 mm, 1 mm depth) and a drilled hole for a temperature sensor were used to ensure an equal temperature distribution over the whole area. Twelve samples have been heated to the dedicated temperature simultaneously and kept there for 24 h.

3.3 Emission Measurements

Direct and delayed emission measurements were performed using a CAS 140CTS from Instrument Systems. To trigger the detection and the 365 nm (Thorlabs, M365 L2) LED, a TGP3122 pulse generator (AIM-TTI Instruments) was used. All measurements were performed in darkness under nitrogen or ambient conditions. The control software SweepMe! was used for automated data acquisition [A. Fischer, F. Kaschura, SweepMe! A

multi-tool measurement software, www.sweep-me.net (accessed: 2021–12–20)].

3.4 Lifetime Measurements

The phosphorescent lifetime was determined using a silicon photodetector PDA100A by Thorlabs. The decay was recorded and fitted using a two-exponential fit resulting in an intensity-averaged lifetime. The prodecure and details can be found in Refs. [41, 52]. The measurement error is ±5 ms.

3.5 PLQY Measurements

The PLQY values were determined using the method proposed by de Mello et al. [53], improved by F. Fries. [49] As excitation source, a 300 W xenon lamp in combination with a monochromator (LOT Quantum Design MSH300) was used. The samples were placed in a calibrated integration sphere (Labsphere RTC-060-SF) and the spectra were acquired with an array spectrometer (CAS 140CT, Instrument Systems).

3.6 GIWAXS Measurements

GIWAXS investigations were performed at the NCD-SWEET beamline at the ALBA synchrotron. An area detector (LX255-HS, Rayonix) was placed approximately 20 cm behind the sample. The beam size was 80 μm horizontally and 30 μm vertically, and the beam energy was 12.4 keV. The incidence angle was 0.12°. The collected images were calibrated using a chromium oxide calibration standard and background-subtracted using background images obtained from a plain quartz sample.

3.7 Film Thickness

Film thickness was determined using a profilometer Veeco Dektak 150 from Bruker. A groove has been cut into the film in the middle of the sample using a cannula. A line scan was done at three different positions and the thickness values were averaged.

4 CONCLUSION

This study compares the phosphorescence performance of differently produced thin films employing all the same RTP emitter. The host polymer, the annealing temperature, and the fabrication technique were varied. Every combination was evaluated with regard to phosphorescence lifetime, PLQY, and P2L ratio. In terms of the host polymer, the most significant change was detected reaching annealing temperatures above the glass transition temperature. PLA, which has the lowest T_G, clearly showed a performance drop above 80 °C annealing temperature. Apart from PLA, reasonable annealing temperatures below T_G do not seem to change the overall phosphorescence performance in case of drop-cast and blade-coated samples. With respect to the fabrication technique, spin-coated films that are thinner by an order of magnitude, showed the poorest performance, while blade-coating and drop-casting yielded comparable results. This behavior might be induced by a higher net excitation intensity in thin films but is not yet fully understood at this stage and subject to further ongoing experiments. Going from thin to thick spin-coated films, the phosphorescence lifetime could be increased by a factor of up to 2.5 (PLA, sc).

DATA AVAILABILITY STATEMENT

The original contributions presented in the study are included in the article/**Supplementary Material**, further inquiries can be directed to the corresponding author.

AUTHOR CONTRIBUTIONS

HT prepared the samples, performed all measurements and wrote the manuscript. TB prepared the thick spin-coated samples. HT and KH did the blade-coating experiment. KH, FT and SM contributed GIWAXS data/analysis, TA, TB, AK, KH, and FT revised the manuscript and helped with data evaluation. SR supervised the project and revised the manuscript.

FUNDING

This work has received funding from the European Social Fund (Project OrgNanoMorph, proposal no. 100382168) and from the European Research Council (ERC) under the European Union's Horizon 2020 research and innovation program (Grant Agreement No. 679213 "BILUM"). The GIWAXS experiments were performed at the BL11 NCDSWEET beamline at ALBA Synchrotron with the collaboration of ALBA staff. The research leading to this result has been supported by the project CALIPSOplus under Grant Agreement 730872 from the EU Framework Program for Research and Innovation HORIZON 2020.

ACKNOWLEDGMENTS

HT and KH acknowledge the funding of the European Social Fund. FT acknowledges financial support from the German Research Foundation (DFG, MA 3342/6-1). AK acknowledges financial support from DFG project HEFOS (grant no. FI 2449/1-1). KH, FT and SM would like to acknowledge support by the German Excellence Initiative via the Cluster of Excellence EXC 1056 "Center for Advancing Electronics Dresden (cfaed)".

SUPPLEMENTARY MATERIAL

The Supplementary Material for this article can be found online at: https://www.frontiersin.org/articles/10.3389/fphy.2022.841413/full#supplementary-material

REFERENCES

1. Reineke S, Baldo MA. Room Temperature Triplet State Spectroscopy of Organic Semiconductors. *Sci Rep* (2015) 4:3797–804. doi:10.1038/srep03797
2. Xu S, Chen R, Zheng C, Huang W. Excited State Modulation for Organic Afterglow: Materials and Applications. *Adv Mater* (2016) 28:9920–40. doi:10.1002/adma.201602604
3. Yan X, Peng H, Xiang Y, Wang J, Yu L, Tao Y, et al. Recent Advances on Host-Guest Material Systems toward Organic Room Temperature Phosphorescence. *Small* (2021) 18:2104073. doi:10.1002/smll.202104073
4. Hirata S. Recent Advances in Materials with Room-Temperature Phosphorescence: Photophysics for Triplet Exciton Stabilization. *Adv Opt Mater* (2017) 5:1700116. doi:10.1002/adom.201700116
5. Ding L, Wang X-d. Luminescent Oxygen-Sensitive Ink to Produce Highly Secured Anticounterfeiting Labels by Inkjet Printing. *J Am Chem Soc* (2020) 142:13558–64. doi:10.1021/jacs.0c05506
6. Gmelch M, Thomas H, Fries F, Reineke S. Programmable Transparent Organic Luminescent Tags. *Sci Adv* (2019) 5:5. doi:10.1126/sciadv.aau7310
7. Li H, Li H, Wang W, Tao Y, Wang S, Yang Q, et al. Stimuli-Responsive Circularly Polarized Organic Ultralong Room Temperature Phosphorescence. *Angew Chem Int Ed* (2020) 59:4756–62. doi:10.1002/anie.201915164
8. Xu Y, Xu R, Wang Z, Zhou Y, Shen Q, Ji W, et al. Recent Advances in Luminescent Materials for Super-resolution Imaging via Stimulated Emission Depletion Nanoscopy. *Chem Soc Rev* (2021) 50:667–90. doi:10.1039/d0cs00676a
9. Jayabharathi J, Goperundevi G, Thanikachalam V, Panimozhi S. Regulation of Singlet and Triplet Excitons in a Single Emission Layer: Efficient Fluorescent/Phosphorescent Hybrid White Organic Light-Emitting Diodes. *ACS Omega* (2019) 4:15030–42. doi:10.1021/acsomega.9b01815
10. Kabe R, Notsuka N, Yoshida K, Adachi C. Afterglow Organic Light-Emitting Diode. *Adv Mater* (2016) 28:655–60. doi:10.1002/adma.201504321
11. Huang Q, Gao H, Yang S, Ding D, Lin Z, Ling Q. Ultrastable and Colorful Afterglow from Organic Luminophores in Amorphous Nanocomposites: Advanced Anti-counterfeiting and *In Vivo* Imaging Application. *Nano Res* (2020) 13:1035–43. doi:10.1007/s12274-020-2740-x
12. Kirch A, Fischer A, Liero M, Fuhrmann J, Glitzky A, Reineke S. Electrothermal Tristability Causes Sudden Burn-In Phenomena in Organic LEDs (Adv. Funct. Mater. 47/2021). *Adv Funct Mater* (2021) 31:2170349. doi:10.1002/adfm.202170349
13. Hirata S, Totani K, Yamashita T, Adachi C, Vacha M. Large Reverse Saturable Absorption under Weak Continuous Incoherent Light. *Nat Mater* (2014) 13:938–46. doi:10.1038/nmat4081
14. Kwon MS, Yu Y, Coburn C, Phillips AW, Chung K, Shanker A, et al. Suppressing Molecular Motions for Enhanced Room-Temperature Phosphorescence of Metal-free Organic Materials. *Nat Commun* (2015) 6:8947. doi:10.1038/ncomms9947
15. Sun Y, Liu S, Sun L, Wu S, Hu G, Pang X, et al. Ultralong Lifetime and Efficient Room Temperature Phosphorescent Carbon Dots through Multi-Confinement Structure Design. *Nat Commun* (2020) 11:5591. doi:10.1038/s41467-020-19422-4
16. Hirata S, Totani K, Zhang J, Yamashita T, Kaji H, Marder SR, et al. Efficient Persistent Room Temperature Phosphorescence in Organic Amorphous Materials under Ambient Conditions. *Adv Funct Mater* (2013) 23:3386–97. doi:10.1002/adfm.201203706
17. Mieno H, Kabe R, Notsuka N, Allendorf MD, Adachi C. Long-Lived Room-Temperature Phosphorescence of Coronene in Zeolitic Imidazolate Framework ZIF-8. *Adv Opt Mater* (2016) 4:1015–21. doi:10.1002/adom.201600103
18. Baroncini M, Bergamini G, Ceroni P. Rigidification or Interaction-Induced Phosphorescence of Organic Molecules. *Chem Commun* (2017) 53:2081–93. doi:10.1039/c6cc09288h
19. Bolton O, Lee K, Kim H-J, Lin KY, Kim J. Activating Efficient Phosphorescence from Purely Organic Materials by crystal Design. *Nat Chem* (2011) 3:205–10. doi:10.1038/nchem.984
20. Hamzehpoor E, Perepichka DF. Crystal Engineering of Room Temperature Phosphorescence in Organic Solids. *Angew Chem Int Ed* (2020) 59:9977–81. doi:10.1002/anie.201913393
21. An Z, Zheng C, Tao Y, Chen R, Shi H, Chen T, et al. Stabilizing Triplet Excited States for Ultralong Organic Phosphorescence. *Nat Mater* (2015) 14:685–90. doi:10.1038/nmat4259
22. Lucenti E, Forni A, Botta C, Carlucci L, Giannini C, Marinotto D, et al. Cyclic Triimidazole Derivatives: Intriguing Examples of Multiple Emissions and Ultralong Phosphorescence at Room Temperature. *Angew Chem Int Ed* (2017) 56:16302–7. doi:10.1002/anie.201710279
23. Gu L, Shi H, Bian L, Gu M, Ling K, Wang X, et al. Colour-tunable Ultra-long Organic Phosphorescence of a Single-Component Molecular crystal. *Nat Photon* (2019) 13:406–11. doi:10.1038/s41566-019-0408-4
24. Bian L, Shi H, Wang X, Ling K, Ma H, Li M, et al. Simultaneously Enhancing Efficiency and Lifetime of Ultralong Organic Phosphorescence Materials by Molecular Self-Assembly. *J Am Chem Soc* (2018) 140:10734–9. doi:10.1021/jacs.8b03867
25. Wang Z, Zhu C-Y, Wei Z-W, Fan Y-N, Pan M. Breathing-Ignited Long Persistent Luminescence in a Resilient Metal-Organic Framework. *Chem Mater* (2020) 32:841–8. doi:10.1021/acs.chemmater.9b04440
26. Ma X, Wang J, Tian H. Assembling-Induced Emission: An Efficient Approach for Amorphous Metal-free Organic Emitting Materials with Room-Temperature Phosphorescence. *Acc Chem Res* (2019) 52:738–48. doi:10.1021/acs.accounts.8b00620
27. DeRosa CA, Samonina-Kosicka J, Fan Z, Hendargo HC, Weitzel DH, Palmer GM, et al. Oxygen Sensing Difluoroboron Dinaphthoylmethane Polylactide. *Macromolecules* (2015) 48:2967–77. doi:10.1021/acs.macromol.5b00394
28. Al-Attar HA, Monkman AP. Room-Temperature Phosphorescence from Films of Isolated Water-Soluble Conjugated Polymers in Hydrogen-Bonded Matrices. *Adv Funct Mater* (2012) 22:3824–32. doi:10.1002/adfm.201200814
29. Ogoshi T, Tsuchida H, Kakuta T, Yamagishi Ta., Taema A, Ono T, et al. Ultralong Room-Temperature Phosphorescence from Amorphous Polymer Poly(Styrene Sulfonic Acid) in Air in the Dry Solid State. *Adv Funct Mater* (2018) 28:1707369. doi:10.1002/adfm.201707369
30. Tang G, Zhang K, Feng T, Tao S, Han M, Li R, et al. One-step Preparation of Silica Microspheres with Super-stable Ultralong Room Temperature Phosphorescence. *J Mater Chem C* (2019) 7:8680–7. doi:10.1039/c9tc02353d
31. Wang C, Chen Y, Hu T, Chang Y, Ran G, Wang M, et al. Color Tunable Room Temperature Phosphorescent Carbon Dot Based Nanocomposites Obtainable from Multiple Carbon Sources via a Molten Salt Method. *Nanoscale* (2019) 11:11967–74. doi:10.1039/c9nr03038g
32. Su Y, Phua SZF, Li Y, Zhou X, Jana D, Liu G, et al. Ultralong Room Temperature Phosphorescence from Amorphous Organic Materials toward Confidential Information Encryption and Decryption. *Sci Adv* (2018) 4:eaas9732. doi:10.1126/sciadv.aas9732
33. Kwon MS, Lee D, Seo S, Jung J, Kim J. Tailoring Intermolecular Interactions for Efficient Room-Temperature Phosphorescence from Purely Organic Materials in Amorphous Polymer Matrices. *Angew Chem Int Ed* (2014) 53:11177–81. doi:10.1002/anie.201404490
34. Lantz KR, Pate R, Stiff-Roberts AD, Duffell AG, Smith ER, Everitt HO. Comparison of Conjugated Polymer Deposition Techniques by Photoluminescence Spectroscopy. *J Vac Sci Technol B* (2009) 27:2227–31. doi:10.1116/1.3222855
35. Bora MÖ. The Influence of Heat Treatment on Scratch Behavior of Polymethylmethacrylate (PMMA). *Tribology Int* (2014) 78:75–83. doi:10.1016/j.triboint.2014.04.030
36. Thomas H, Fries F, Gmelch M, Bärschneider T, Kroll M, Vavaleskou T, et al. Purely Organic Microparticles Showing Ultralong Room Temperature Phosphorescence. *ACS Omega* (2021) 6:13087–93. doi:10.1021/acsomega.1c00785
37. Kirch A, Gmelch M, Reineke S. Simultaneous Singlet-Singlet and Triplet-Singlet Förster Resonance Energy Transfer from a Single Donor Material. *J Phys Chem Lett* (2019) 10:310–5. doi:10.1021/acs.jpclett.8b03668
38. Reineke S, Lindner F, Schwartz G, Seidler N, Walzer K, Lüssem B, et al. White Organic Light-Emitting Diodes with Fluorescent Tube Efficiency. *Nature* (2009) 459:234–8. doi:10.1038/nature08003
39. Fries F, Fröbel M, Lenk S, Reineke S. Transparent and Color-Tunable Organic Light-Emitting Diodes with Highly Balanced Emission to Both Sides. *Org Electro* (2017) 41:315–8. doi:10.1016/j.orgel.2016.11.022

40. Adamovich VI, Cordero SR, Djurovich PI, Tamayo A, Thompson ME, D'Andrade BW, et al. New Charge-Carrier Blocking Materials for High Efficiency OLEDs. *Org Electro* (2003) 4:77–87. doi:10.1016/j.orgel.2003.08.003
41. Salas Redondo C, Kleine P, Roszeitis K, Achenbach T, Kroll M, Thomschke M, et al. Interplay of Fluorescence and Phosphorescence in Organic Biluminescent Emitters. *J Phys Chem C* (2017) 121:14946–53. doi:10.1021/acs.jpcc.7b04529
42. Wilson DF. Oxygen Dependent Quenching of Phosphorescence: A Perspective. *Adv Exp Med Biol* (1992) 317:195–201. doi:10.1007/978-1-4615-3428-0_20
43. Borisov SM. CHAPTER 1. Fundamentals of Quenched Phosphorescence O2 Sensing and Rational Design of Sensor Materials. In: *Quenched-phosphorescence Detection of Molecular Oxygen: Applications in Life Science*. Cambridge, MA: Royal Society of Chemistry (2018). p. 1–18. doi:10.1039/9781788013451-00001
44. Köhler A, Bässler H. *Decay of Excitations" in: Electronic Processes in Organic Semiconductors*. Weinheim: Wiley-VCH Verlag GmbH and Co. KGaA (2015). p. 287
45. Chang M, Lim G, Park B, Reichmanis E. Control of Molecular Ordering, Alignment, and Charge Transport in Solution-Processed Conjugated Polymer Thin Films. *Polymers* (2017) 9:212–37. doi:10.3390/polym9060212
46. Gu X, Shaw L, Gu K, Toney MF, Bao Z. The Meniscus-Guided Deposition of Semiconducting Polymers. *Nat Commun* (2018) 9:534. doi:10.1038/s41467-018-02833-9
47. Tomkeviciene A, Dabulienė A, Matulaitis T, Guzauskas M, Andruleviciene V, Grazulevicius JV, et al. Bipolar Thianthrene Derivatives Exhibiting Room Temperature Phosphorescence for Oxygen Sensing. *Dyes Pigm* (2019) 170: 107605. doi:10.1016/j.dyepig.2019.107605
48. Gmelch M, Achenbach T, Tomkeviciene A, Reineke S. High-Speed and Continuous-Wave Programmable Luminescent Tags Based on Exclusive Room Temperature Phosphorescence (RTP). *Adv Sci* (2021) 8:2102104. doi:10.1002/advs.202102104
49. Fries F, Reineke S. Statistical Treatment of Photoluminescence Quantum Yield Measurements. *Sci Rep* (2019) 9:15638. doi:10.1038/s41598-019-51718-4
50. Thomas H, Pastoetter DL, Gmelch M, Achenbach T, Schlögl A, Louis M, et al. Aromatic Phosphonates: A Novel Group of Emitters Showing Blue Ultralong Room Temperature Phosphorescence. *Adv Mater* (2020) 32:2000880. doi:10.1002/adma.202000880
51. Ito Y, Virkar AA, Mannsfeld S, Oh JH, Toney M, Locklin J, et al. Crystalline Ultrasmooth Self-Assembled Monolayers of Alkylsilanes for Organic Field-Effect Transistors. *J Am Chem Soc* (2009) 131:9396–404. doi:10.1021/ja9029957
52. Lakowicz JR. *Principles of Fluorescence Spectroscopy*. New York, NY: Springer Science+Business Media, LLC (1983).
53. de Mello JC, Wittmann HF, Friend RH. An Improved Experimental Determination of External Photoluminescence Quantum Efficiency. *Adv Mater* (1997) 9:230–2. doi:10.1002/adma.19970090308

Conflict of Interest: The authors declare that the research was conducted in the absence of any commercial or financial relationships that could be construed as a potential conflict of interest.

Publisher's Note: All claims expressed in this article are solely those of the authors and do not necessarily represent those of their affiliated organizations, or those of the publisher, the editors and the reviewers. Any product that may be evaluated in this article, or claim that may be made by its manufacturer, is not guaranteed or endorsed by the publisher.